Quasiperiodicity of some quasars important to ICRF-Gaia CRF link

Miljana D. Jovanović, Goran Damljanović
Astronomical observatory, Volgina 7, 11060 Belgrade, Serbia
miljana@aob.rs
(Submitted on 30.09.2019. Accepted on 05.11.2019)

Abstract. The ESA/Gaia astrometric mission will provide a catalogue of about one billion stars and 600 000 quasars – QSOs, some of them could be the basis of a new optical reference frame. To link the future Gaia CRF (at optical wavelength) with the ICRF (based on the VLBI observations of quasars at radio wavelengths) it is required to observe a set of QSOs which are visible in the optical domain. Only about 10% of the ICRF sources ($\sim$ 70 sources) are suitable for this task. Photometry stability of 47 candidate sources (Bourda et al. 2011) is of importance for astrometry and mentioned link. Our observations of these sources have been carried out by using three telescopes: two of them at the Astronomical Station Vidojevica (of the Astronomical Observatory of Belgrade) and the third one at the Rozhen National Astronomical Observatory (Bulgaria). We tested brightness variability of five candidate sources and their suitable comparison stars using the F–test. Only the brightness of one object does not show variability. For the four remaining objects we used the method of Least Squares to estimate sinusoidal parameters of quasiperiods of their light curves. The results of the mentioned brightness analysis of 5 objects and their 30 comparison stars (for the period July 2016 until August 2019) are presented here.
Key words: Galaxies – active, Methods – data analysis, Techniques – photometric

Introduction

The International Celestial Reference Frame 3 (ICRF3) was adopted by the International Astronomical Union in August 2018. The ICRF3, unlike its first versions ICRF (Ma et al. 1998) and ICRF2 (Fey et al. 2015), is a multifrequency catalogue containing source coordinates observed at three different frequencies. The ICRF3 contains coordinates of 4536 extragalactic radio sources in J2000.0, determined by using Very Long Baseline Interferometry – VLBI; 303 of which, uniformly distributed on the sky, are identified as defining sources and as such serve to define the axes of the frame (http://hpiers.obspm.fr/icrs-pc/newwww/icrf/icrf3-ReadMe.txt).

The Global Astrometric Interferometer for Astrophysics (Gaia) satellite of the European Space Agency was launched in December 2013. The second data release (DR2) of the Gaia mission has been made publicly available in April 2018 (Gaia Collaboration et al. 2018). The Gaia DR2 provides 5 complete astrometric parameters (positions, parallaxes, and proper motions) for more than 1.3 billion sources (of which 600 000 are QSOs – quasars). A new optical Gaia Celestial Reference Frame (Gaia CRF) will be at the same level of accuracy as the ICRF. The orientation of Gaia CRF axes (fixed with respect to distant extragalactic objects) should coincide with the ICRF as much as possible. The link between these two frames will be established by using Gaia observations of compact extragalactic ICRF objects with accurate radio positions. For this link are suitable only about 70 ICRF sources. In the paper of Bourda et al. (2011), 47 extragalactic radio sources (out of the ICRF list) with high astrometric quality have been identified as potential candidates for the link. We started with observations

of these candidate sources in July 2016. These sources are Active Galactic Nuclei (AGNs), most of them are QSO type (30 sources), the others are BL Lacertae – BL Lac (15) and Seyfert galaxies type 1 – Sy 1 (2).

An AGN represents a phase in the life of a galaxy with presence of energetic phenomena in the galactic center, which cannot be attributed directly to stars. Variations in the optical and radio bands are very important to understand their physical properties. Time scale variability is divided into: less than a day is Intra-Day Variability – IDV; with range of a few days to a few months is Short Term Variability – STV; and from a few months to several years is Long Term Variability – LTV (Gupta 2014). Correlation between the brightness variability and astrometric positions of QSOs in some cases is discussed in several papers Taris et al. (2011, 2016); Popović et al. (2012). The sources with more stable brightness are preferred for the link between Gaia CRF and ICRF. It is necessary to monitor brightness stability of these sources over a longer period of time. Some results of STV of presented objects are given in Taris et al. (2018).

The subject of this paper is the investigation of the quasiperiodicity of five AGNs which have been observed for about 3 years. The objects 1535+231 and 1556+335 are type QSOs and 1607+604, 1722+119, and 1741+597 – BL Lac.

1. Observations and Data Reduction

The observations were made by using three different telescopes. Two telescopes (60-cm Cassegrain and the 1.4-m Ritchey-Chrétien) are located at Astronomical Station Vidojevica (ASV) of the Astronomical Observatory of Belgrade (longitude $\lambda = 21^{\circ}5$E, latitude $\varphi = 43^{\circ}1$N, and altitude ~ 1150 m). The third, 2-m Ritchey-Chrétien telescope is located at the Rozhen NAO in Bulgaria ($\lambda = 24^{\circ}7$E, $\varphi = 41^{\circ}7$N, altitude 1730 m). During this observational period CCD cameras of five different types were mounted on the telescopes. Apogee Alta E47 (CCD resolution is 1024×1024, pixel size 13×13 μm) was mounted on 60-cm ASV telescope (pixel scale $0\farcs450$/px, and field of view $7\farcm6 \times 7\farcm6$). CCD cameras with the same type Andor iKon-L (2048×2048, 13.5×13.5 μm) were mounted on 1.4-m ASV and 2-m Rozhen telescopes ($0\farcs244$/px, $8\farcm3 \times 8\farcm3$ with focal reducer $0\farcs391$/px, $13\farcm3 \times 13\farcm3$; $0\farcs176$/px, $6\farcm0 \times 6\farcm0$). Characteristics of CCD cameras SBIG ST10 XME mounted on 60-cm ASV, VersArray 1300B on 2-m Rozhen, and Apogee Alta U42 on 60-cm and 1.4-m ASV telescopes are presented in Damljanović et al. (2014).

Most frequently two CCD images per V and R filter have been obtained. The CCD images were reduced (bias, dark, flat, hot and dead pixels, and cosmic rays) by using Image Reduction and Analysis Facility – IRAF scripting language (ascl:9911.002) (Tody 1986, 1993).

MaxIm DL software tool for differential photometry was used for calculating objects brightness. For this purpose several stars located in the vicinity of the objects were chosen: two comparison stars with brightness similar to that of the object, and a few control stars. The stars were selected from the Sloan Digital Sky Survey Data Release 14 (SDSS DR14) catalogue

(Abolfathi et al. 2018), with the exception of 1722+119 from Doroshenko et al. (2014).

The stars were selected using the following criteria: non-variable, avoiding bright, faint, very blue or red stars, etc. The transformation from SDSS PSF *ugriz* (point spread function u, g, r, i, and z) magnitudes to the Johnson-Cousins *BVRI* (B, V, R, and I) ones was performed using the equations (Chonis and Gaskel 2008):

$$B = g + (0.327 \pm 0.047)(g - r) + (0.216 \pm 0.027), \quad (1)$$
$$V = g - (0.587 \pm 0.022)(g - r) - (0.011 \pm 0.013), \quad (2)$$
$$R = r - (0.272 \pm 0.092)(r - i) - (0.159 \pm 0.022), \quad (3)$$
$$I = i - (0.337 \pm 0.191)(r - i) - (0.370 \pm 0.041), \quad (4)$$

where $14.5 < g, r, i < 19.5$, $0.08 < r - i < 0.5$ and $0.2 < g - r < 1.4$.

The presented objects were observed for about 1130 days (∼3 years). During this period, photometrically, the most stable object was quasar 1556+335, with redshift (z) 1.653476. Its magnitudes are close to the average value in both filters. The magnitudes of quasar 1535+231 (z = 0.462524) and BL Lac 1607+604 (z = 0.178) have variations less than 1 magnitude. Their extremal magnitudes (maximum and minimum values) are 18.132 and 18.702 in V filter, 17.796 and 18.476 in R (1535+231), and 17.304 and 17.690, 16.886 and 17.148 (1607+604), respectively. Unlike them, the brightness of BL Lac objects 1741+597 ($z = 0.4$) and 1722+119 ($z = 0.018$) changed by about 1.6 and 2 magnitudes in both filters. Because of this remarkable variability the standard deviations of the obtained magnitudes are larger than for the other objects. The magnitude range is from 16.858 to 18.470 in V, and 16.479 to 18.171 in R (1741+597), and 14.888 and 16.780, 14.372 and 16.344 (1722+119), respectively.

The analysis of the brightness variability of 1722+119 is presented in two papers. In Taris et al. (2018) is presented a period of 35 days in G band, and in Rani et al. (2009), a period of about one year in X-ray was explained as observational artifact.

The redshifts were taken from the NASA/IPAC Extragalactic Database - NED (https://ned.ipac.caltech.edu/), and objects type from SIMBAD Astronomical Database. Finding charts of the objects with their comparison and control stars are presented in Jovanović et al. (2018).

In Table 1 are listed the coordinates of the objects and their comparison (A and B) and control stars, calculated $V_{\rm C}$ and $R_{\rm C}$ magnitudes using Eqs. (1) – (4) for stars from SDSS DR14 and those from Doroshenko et al. (2014), together with average obtained magnitudes $V_{\rm O}$ and $R_{\rm O}$ of the objects and the stars, for the period July 2016 – August 2019.

The standard deviations of the comparison and control stars for all the objects are of the order of about of 0.01 (see Table 1), which is in line with groundbased relative photometry.

As an example, the light curves of object 1722+119 (black line), and its comparison (2, and C4 – red) and control stars (C2, C3, 1, 5, 9, and 10 – blue lines) are given in Fig. 1. Variability of the object (confirmed using

F–test) is evident from the light curve, especially in comparison with the light curves of the comparison and control stars.

Table 1. Coordinates, V and R magnitudes with standard errors of the objects and their comparison and control stars.

Object No.	$\alpha_{J2000.0}(^\circ)$	$\delta_{J2000.0}(^\circ)$	$V_C \pm \sigma_{V_C}$(mag)	$R_C \pm \sigma_{R_C}$(mag)	$V_O \pm \sigma_{V_O}$(mag)	$R_O \pm \sigma_{R_O}$(mag)
1535+231	234.31041	23.01126			18.375 ±0.197	18.099 ±0.214
2 (A)	234.31491	23.01831	17.200 ± 0.031	16.658 ± 0.038	17.213 ±0.024	16.693 ±0.036
3	234.30004	23.02486	15.983 ± 0.030	15.633 ± 0.031	16.000 ±0.024	15.656 ±0.030
4 (B)	234.25178	23.01917	16.232 ± 0.024	15.867 ± 0.029	16.227 ±0.010	15.851 ±0.017
7	234.29312	22.96096	16.470 ± 0.027	15.973 ± 0.036	16.452 ±0.026	15.958 ±0.021
8	234.35917	23.01592	15.860 ± 0.035	15.149 ± 0.050	15.841 ±0.024	15.142 ±0.028
1556+335	239.72993	33.38851			17.501 ±0.048	17.020 ±0.040
2 (A)	239.71950	33.39110	17.336 ± 0.030	16.850 ± 0.038	17.344 ±0.031	16.895 ±0.032
3 (B)	239.69035	33.40959	16.381 ± 0.027	16.095 ± 0.030	16.378 ±0.013	16.074 ±0.015
5	239.76798	33.38778	16.271 ± 0.030	15.916 ± 0.031	16.289 ±0.025	15.936 ±0.022
6	239.74562	33.39003	16.198 ± 0.030	15.825 ± 0.031	16.225 ±0.022	15.876 ±0.021
7	239.74317	33.37370	15.552 ± 0.030	15.188 ± 0.031	15.568 ±0.023	15.223 ±0.017
8	239.73398	33.37219	15.743 ± 0.040	14.897 ± 0.064	15.756 ±0.045	14.966 ±0.016
1607+604	242.08560	60.30783			17.479 ±0.118	17.045 ±0.085
2	242.02882	60.28951	17.068 ± 0.027	16.619 ± 0.031	17.074 ±0.038	16.622 ±0.039
3 (A)	242.02526	60.31162	16.864 ± 0.025	16.423 ± 0.032	16.896 ±0.032	16.462 ±0.027
4	241.97352	60.35552	15.195 ± 0.025	14.781 ± 0.031	15.173 ±0.045	14.742 ±0.035
5 (B)	242.09638	60.34816	15.630 ± 0.031	14.965 ± 0.044	15.620 ±0.010	14.955 ±0.007
7	242.16854	60.37746	16.856 ± 0.024	16.467 ± 0.031	16.844 ±0.032	16.411 ±0.049
1722+119	261.26810	11.87096			15.515 ±0.604	15.009 ±0.601
1	261.31208	11.89125	13.445 ± 0.009	12.848 ± 0.010	13.448 ±0.034	12.856 ±0.025
2 (A)	261.30458	11.86519	14.823 ± 0.008	14.691 ± 0.012	14.828 ±0.008	14.688 ±0.004
5	261.25667	11.91311	15.873 ± 0.010	15.385 ± 0.016	15.866 ±0.047	15.379 ±0.022
9	261.23333	11.87083	15.809 ± 0.008	15.332 ± 0.014	15.803 ±0.023	15.340 ±0.019
10	261.23875	11.87083	16.142 ± 0.011	15.699 ± 0.019	16.140 ±0.024	15.713 ±0.021
C2	261.27167	11.86997	13.173 ± 0.005	12.570 ± 0.006	13.188 ±0.038	12.631 ±0.028
C3	261.24375	11.86636	14.078 ± 0.012	13.600 ± 0.008	14.087 ±0.022	13.631 ±0.017
C4 (B)	261.28958	11.85344	15.665 ± 0.009	15.164 ± 0.013	15.654 ±0.017	15.169 ±0.007
1741+597	265.63334	59.75186			17.945 ±0.371	17.545 ±0.376
2	265.62329	59.75176	15.565 ± 0.029	15.204 ± 0.054	15.619 ±0.032	15.290 ±0.042
3 (A)	265.57081	59.75387	16.673 ± 0.029	16.314 ± 0.053	16.678 ±0.014	16.331 ±0.016
4	265.68412	59.76861	16.376 ± 0.034	15.795 ± 0.067	16.408 ±0.029	15.840 ±0.024
5	265.61457	59.79547	16.154 ± 0.031	15.704 ± 0.056	16.187 ±0.040	15.753 ±0.024
6	265.68288	59.71901	16.126 ± 0.038	15.684 ± 0.064	16.137 ±0.023	15.696 ±0.022
7 (B)	265.59766	59.71686	16.633 ± 0.039	16.124 ± 0.074	16.628 ±0.014	16.110 ±0.013

Note. (A), (B) refer to comparison stars.

2. Methods and Results

The 3–σ rule was used to reject some data. After that, the Shapiro-Wilk test of normality was used, and it is concluded that tests which require normal data distribution can be applied.

2.1. F–test

We used the F–test to determine the presence in the brightness variability of objects and control stars (de Diego 2010, Gupta et al. 2017). The variances of the two data sets were tested using three hypotheses:
1) H_1: $Var(\mathrm{O-A}) = Var(\mathrm{O-B})$, alternative: H_{a1}: $Var(\mathrm{O-A}) > Var(\mathrm{O-B})$,
2) H_2: $Var(\mathrm{O-A}) = Var(\mathrm{A-B})$, alternative: H_{a2}: $Var(\mathrm{O-A}) > Var(\mathrm{A-B})$,

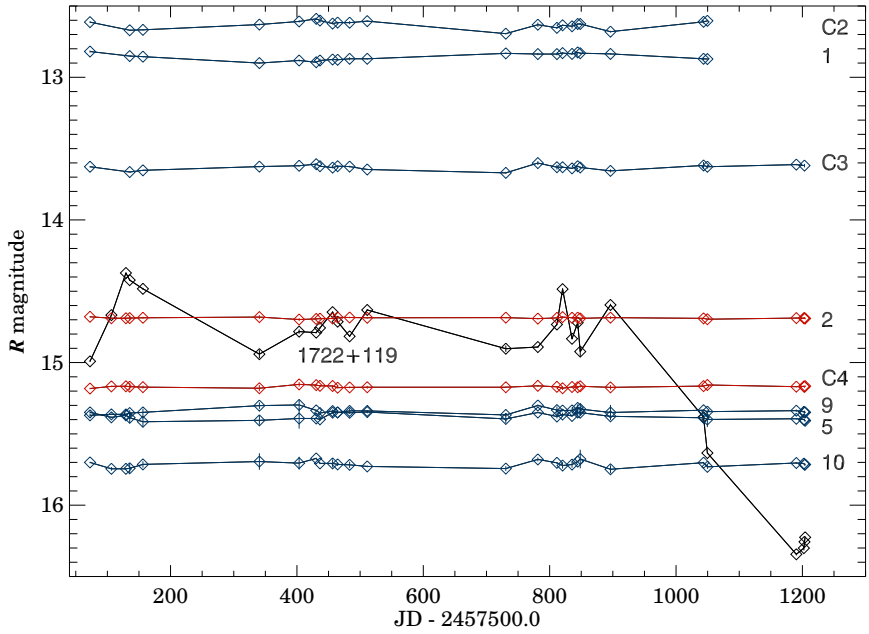

Fig. 1. The light curves 1722+119 and its comparison and control stars from July 2016 until August 2019.

3) H_3: $Var(\mathrm{O}-\mathrm{B}) = Var(\mathrm{A}-\mathrm{B})$, alternative: H_{a3}: $Var(\mathrm{O}-\mathrm{B}) > Var(\mathrm{A}-\mathrm{B})$.

Test statistics which correspond to these hypotheses are: $F_1 = \frac{Var(\mathrm{O}-\mathrm{A})}{Var(\mathrm{O}-\mathrm{B})}$, $F_2 = \frac{Var(\mathrm{O}-\mathrm{A})}{Var(\mathrm{A}-\mathrm{B})}$, and $F_3 = \frac{Var(\mathrm{O}-\mathrm{B})}{Var(\mathrm{A}-\mathrm{B})}$. Designations $Var(\mathrm{O}-\mathrm{A})$, $Var(\mathrm{O}-\mathrm{B})$, and $Var(\mathrm{A}-\mathrm{B})$ refer to variances of differences of magnitudes between object and comparison star A, the object and comparison star B, and comparison star A and B, respectively.

The F_i (i =1, 2, 3) values were compared with the critical values F_c, obtained for significance level set (α) 0.05, 0.01, and 0.001, and number of points (N). If the F_i value is greater than the critical one, the null hypotheses H_i can be discarded. It is expected that variances $Var(\mathrm{O}-\mathrm{A})$ and $Var(\mathrm{O}-\mathrm{B})$ should be close to each other (F_1 value should be around 1). If the brightness is changeable it should be in the same manner for both comparison stars, because they are stable a priori. If F_2 and F_3 are greater than the critical value F_c for significance level of 0.05, the object is considered variable. In the same manner brightness of each control star was investigated.

As a result, the test shows that four objects are variabile in both filters. The non-variable object (1556+335) has F_i values almost equal to 1: F_1 =1.11, F_2 =1.34, F_3 =1.49 in V filter, and F_1 =1.23, F_2 =1.22, F_3 =1.01

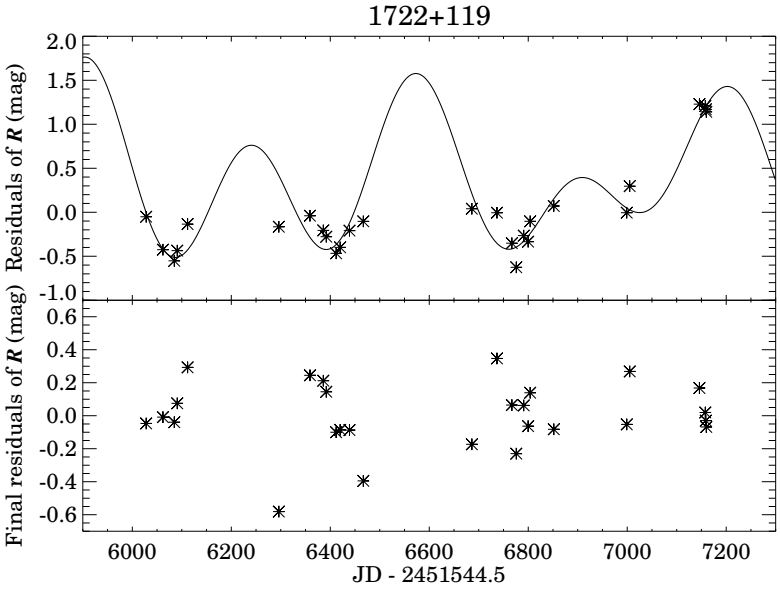

Fig. 2. The LS fit of the light curve of 1722+119 in R band, and final residuals.

in R filter. The critical value is F_c =2.17 for N =20 in V, and F_c =1.93 for N =27 in R.

Four variable objects have F_1 values around 1 as it is expected, but F_2 and F_3 are greater than the critical value. For these objects, F_2, F_3, number of data points N, and critical values F_c (for N and $\alpha = 0.05$) are listed in Table 2 for both filters. The values for 1722+119, and 1741+597 are noticeable as sufficiently high since their brightness variability is significant.

The test shows that the brightness of control stars is non-variable.

2.2. Method of Least Squares

The method of Least Squares (LS) was used for sinusoidal parameters estimations (amplitude and phase) in line with suitable period:

$$f(t) = A\sin(\omega t + \varphi) + f_0, \tag{5}$$

where A is amplitude (in magnitudes), φ phase (in radians), ω angular velocity (in radians per days), f_0 intercept (in magnitudes), and t epoch of observation (in days).

Function $f(t)$ can be expanded as:

$$f(t) = A\cos(\varphi)\sin(\omega t) + A\sin(\varphi)\cos(\omega t) + f_0 = a_0x_0 + a_1x_1 + a_2, \tag{6}$$

Table 2. The F–test results.

Object	Filter	N	F_2, F_3	F_c
1535+231	V	20	31.39, 36.23	2.17
	R	24	15.08, 17.14	2.01
1607+604	V	23	8.19, 8.45	2.05
	R	27	6.72, 6.60	1.93
1722+119	V	25	603.04, 579.63	1.98
	R	27	2794.40, 2813.14	1.93
1741+597	V	34	179.10, 184.68	1.79
	R	40	176.33, 179.57	1.70

where $a_0 = A\cos(\varphi)$, $a_1 = A\sin(\varphi)$, $a_2 = f_0$, $x_0 = \sin(\omega t)$ and $x_1 = \cos(\omega t)$.

Using the Least Squares (LS) three-parameter fitting method we estimated coefficients a_i $(i = 0, 1, 2)$ for a given set of periods P_j $(\omega_j = \frac{2\pi}{P_j})$. The period range is from 0.3 years (in agreement with the Nyquist frequency) to 12 years (3 years is quarter of 12 years), and the step is 0.1 years. The standard error of the estimate σ_0 was calculated using equation:

$$\sigma_0 = \sqrt{\frac{\sum(Y - f)^2}{N - 3}}, \tag{7}$$

where f are LS fitting values, and N the number of data Y. Coefficients a_i $(i = 0, 1, 2)$ are determined for period P for which σ_0 has a minimum value. This procedure was repeated, if more than one local minima was detected. The amplitude and phase were calculated using equations:

$$A = \sqrt{a_0^2 + a_1^2}, \tag{8}$$

$$\varphi = \arctan(a_1/a_0). \tag{9}$$

The method of LS was used to determine periods, amplitude and phase in brightness variability for variable objects. In case of almost all objects, local minima of σ_0 are present for periods around 0.5 years and 1 years, and this is probably observational artifact (Rani 2009). Because of that, these variations were subtracted from the data. The calculated amplitudes for P =0.5, and 1.0 years for objects 1535+231, 1607+604, and 1741+597 are in range from 0.019 mag to 0.181 mag. 1722+119 has remarkable amplitudes in the both filters 0.349 mag in V, and 0.332 mag in R filter of semiannual, and 0.183 in V and 0.255 in R of annual period. After removing these variations from the data, the LS method was repeated on the residuals. The results are presented in Table 3 (amplitude A, phase φ, periods P referred to epoch J2000.0, and standard errors σ_0). For some objects, quasiperiods are slightly different for the two filters because of different number N of data. With continued observations more data in the future will provide more precise results.

An example of the LS fit on residuals (without semiannual and annual variations) of R magnitudes for 1722+119 is given in Fig. 2. The obtained quasiperiods are 0.9, 1.1, and 1.7 years. After removing these three sinusoids, the final residuals are presented in the same figure (lower panel).

To analyse the presence of systematic errors in the final residuals (quasiperiod variations are removed, too) Abbe's criterion was used according to Djurović (1979), Malkin (2013). The analysis was performed for significance level set: 0.05, 0.01, and 0.001. For all objects the Abbe statistic $\gamma(N)$ was greater than the critical value $\gamma_0(N)$ for significance level $\alpha = 0.01$. The residuals could be explained with random variations and the hypothesis that there is no trend in residuals can be accepted. As an example, for object 1722+119 (with $N = 27$ points in R), the value $\gamma(N) = 1.119$ is greater than the critical value $\gamma_0(N) = 0.577$ (for $\alpha = 0.01$).

Table 3. The amplitudes and phases (for epoch J2000.0) of the obtained quasiperiods for 1535+231, 1607+604, 1722+119, and 1741+597.

Object	Filter	σ_0 (mag)	$A \pm \sigma_A$ (mag)	$\varphi \pm \sigma_\varphi(^\circ)$	P (y)
1535+231	V	±0.09	0.068 ± 0.019	61.629 ±23.925	0.6
		±0.14	0.184 ± 0.029	233.756 ±13.742	0.8
		±0.11	0.117 ± 0.022	139.972 ±16.313	1.4
	R	±0.11	0.102 ± 0.020	69.789 ±17.216	0.6
		±0.16	0.193 ± 0.029	229.316 ±13.351	0.8
		±0.13	0.112 ± 0.025	120.225 ±19.245	1.4
1607+604	V	±0.06	0.065 ± 0.012	98.602 ±15.964	1.2
		±0.07	0.081 ± 0.014	281.611 ±14.621	2.3
	R	±0.04	0.078 ± 0.008	289.878 ± 8.904	3.1
1722+119	V	±0.24	0.406 ± 0.044	146.370 ± 9.538	0.7
		±0.36	0.609 ± 0.066	119.573 ± 9.545	1.4
		±0.19	0.250 ± 0.035	182.696 ±12.335	2.2
	R	±0.42	0.704 ± 0.074	101.997 ± 9.203	0.9
		±0.21	0.225 ± 0.038	232.089 ±14.783	1.1
		±0.26	0.515 ± 0.046	251.201 ± 7.795	1.7
1741+597	V	±0.19	0.176 ± 0.031	274.989 ±15.402	0.7
		±0.23	0.213 ± 0.037	317.887 ±15.285	0.9
		±0.29	0.254 ± 0.046	258.820 ±15.808	1.3
	R	±0.32	0.249 ± 0.047	314.964 ±16.601	0.9
		±0.23	0.276 ± 0.034	170.832 ±10.787	1.2
		±0.22	0.125 ± 0.032	100.722 ±22.146	1.7

Conclusion

In this paper are presented monitoring observations of five objects (3 BL Lac and 2 QSOs) in V and R bands during a period of about 3 years. We applied F–test to test systematic brightness variability. The test shows that four objects are variable and for these the amplitude and phase of the sinusoidal curve are estimated using the method of LS. Brightness variabilities with semiannual and annual periods are detected for almost all presented

objects, and they are observational artifact. Only for 1722+119 it could be a real variability with amplitude of semiannual period of about 0.3 mag and annual 0.2 mag in both bands. In Table 3 quasiperiodic variations for the variable objects are presented. Their periods are from 0.6 to 2.3 years. In both filters some of them are with the same (1535+231) or nearly the same value (1722+119, and 1741+597). The different periods in bands could be due to different numbers of points in these filters. During our observational period July 2016 – August 2019, only one object (1556+335) did not show brightness variability.

The calculated V and R magnitudes ($V_{\rm C}$ and $R_{\rm C}$) of all comparison and control stars are in a good agreement with the observed ones ($V_{\rm O}$ and $R_{\rm O}$) in line with their standard errors (see Table 1). After analysis of the stars brightness variability, significant changes were not detected, and we consider that they are suitable for photometric measurements.

It is necessary to proceed with further observations in order to investigate quasiperiods of less than 0.3 years, and greater than several years, and to more precisely determine the variations of amplitude and phase.

Acknowledgments: This work is part of the project 176011 "Dynamics and kinematics of celestial bodies and systems" supported by the Ministry of Education, Science and Technological Development of the Republic of Serbia. The authors acknowledge the observing grant support from the Institute of Astronomy and NAO, BAS, via joint research project "Study of ICRF radio-sources and fast variable astronomical objects" for the period 2017-2019. Funding for the Sloan Digital Sky Survey IV has been provided by the Alfred P. Sloan Foundation, the U.S. Department of Energy Office of Science, and the Participating Institutions. SDSS-IV acknowledges support and resources from the Center for High-Performance Computing at the University of Utah. The SDSS web site is www.sdss.org.

References

Abolfathi, B., Aguado, D. S., Aguilar, G., et al.: 2018, *Astrophys. J. Suppl. Ser.*, 235, 42.
Bourda, G., Collioud, A., Charlot, P., Porcas, R., Garrington, S.: 2011, *Astron. Astrophys.*, 526, A102.
Chonis, T. S. and Gaskel, M. C.: 2008, *Astron. J.*, 135, 264.
Damljanović, G., Vince, O., Boeva, S.,: 2014, *Serb. Astron. J., p.85–93*, 188.
De Diego, J. A.: 2010, *Astron. J.*, 139, 1269.
Djurović, D.: 1979, *Mathematical treatment of the astronomical observations*, University of Belgrade (in Serbian).
Doroshenko, V. T., Efimov, Yu. S., Borman, G. A., Pulatova, N. G.: 2014, *Astrophysics*, 57, 176.
Fey, A. L., Gordon, D., Jacobs, C. S., et al.: 2015, *Astron. J.*, 150, 58.
Gaia Collaboration, Mignard, F., Klioner, S. A., Lindegren, L., et al.: 2018, *Astron. Astrophys.*, 616, A14.
Gupta, A. C.: 2014, *J. Astrophys. Astr.*, 35, 307.
Gupta, A. C., Agarwal, A., Mishra, A., et al.: 2017, *Mon. Not. R. Astron. Soc.*, 465, 4423.
Jovanović, M. D., Damljanović, G., Vince, O.: 2018, *Publ. Astron. Soc. "Rudjer Bošković", p.197–205*, 18, 307.
Ma, C., Arias, E. F., Eubanks, T. M., et al.: 1998, *Astron. J.*, 116, 516.
Malkin, Z. M.: 2013, *Astron. Rep.*, 57, 128.
Popović, L. Č., Jovanović, P., Stalevski, M., et al: 2012, *Astron. Astrophys.*, 538, A107.
Taris, F., Souchay, J., Andrei, A. H., et al.: 2011, *Astron. Astrophys.*, 526, A25.
Taris, F., Damljanovic, G., Andrei, A., et al.: 2018, *Astron. Astrophys.*, 611, A52.
Tody, D.: 1986, *Proceedings SPIE Instrumentation in Astronomy VI*, ed. D.L. Crawford, 627, 733.
Tody, D.: 1993, *Astronomical Data Analysis Software and Systems II, A.S.P. Conference Ser.*, eds. R.J. Hanisch, R.J.V. Brissenden, & J. Barnes, 52, 173.